LEVEL II

ON THE SOLUTION OF NONLINEAR FREE-SURFACE PROBLEMS BY SURFACE-SINGULARITY TECHNIQUES

by

John L. Hess

John L. Hess, Associates

July 10, 1978

Report No. 2

This research was carried out under the Naval Ship Systems Command General Hydromechanics Research Program Subproject SR 023 01 01 adminstered by the Naval Ship Research and Development Center Contract N00014-76-C-0337

APPROVED FOR PUBLIC RELEASE;
DISTRIBUTION UNLIMITED

ON THE SOLUTION OF NONLINEAR FREE-SURFACE PROBLEMS BY SURFACE-SINGULARITY TECHNIQUES

by

John L. Hess

John L. Hess, Associates

July 10, 1978

Report No. 2

This research was carried out under the Naval Ship Systems Command General Hydromechanics Research Program Subproject SR 023 01 01 adminstered by the Naval Ship Research and Development Center Contract N00014-76-C-0337

1.0 ABSTRACT

This report describes an attempt to solve the two-dimensional problem of a body performing steady translation near a free surface. The aim was to solve the problem in its full generality without any linearizations or small-perturbation assumptions. The method of solution is based on iterative use of the well-known surface singularity technique and thus, if successful, the method could be generalized to three dimensions. At each stage of the procedure the free-surface shape is assumed known and the singularity strength adjusted to satisfy the constant-pressure boundary condition. In general, the normal velocity on the free surface is not zero. The free-surface shape is then altered by some algorithm, and the procedure is iterated to obtain zero normal velocity. The key to this approach is the iterative algorithm. Various algorithms were tested by applying them to the problem of a submerged point vortex and comparing the free-surface shape obtained in convergent cases with published results. After considerable experimentation, a procedure was devised that gives very good results as long as the wave heights are not too large. For large wave heights, convergence could not be obtained, and some as yet undiscovered change in the method is needed.

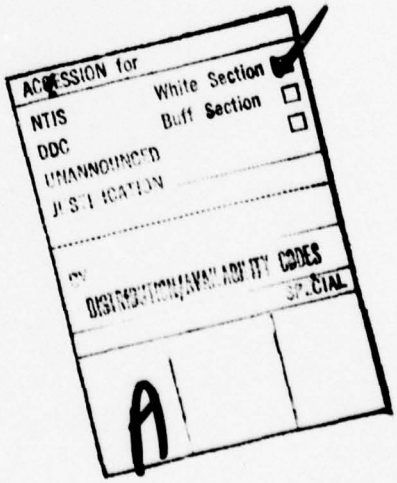

2.0 TABLE OF CONTENTS

1.0 Abstract 1

2.0 Table of Contents 2

3.0 Index of Figures 3

4.0 Principal Notation 4

5.0 Introduction 5

6.0 General Description of the Flow Problem 6

7.0 The Prototype Problem 9

8.0 The Surface Singularity Method 11

9.0 Iteration Algorithms 13

9.1 Local Algorithms 13
9.2 Global Algorithms 13

10.0 First-Order Representation of the Free Surface with No Flat 16

11.0 First-Order Representation of the Free Surface with an Initial Flat. 17

12.0 A Nonuniqueness Due to Numerical Inaccuracy 19

13.0 The Higher-Order Procedure 20

14.0 Larger Values of Vortex Strength 21

15.0 Attempts to Improve the Calculation Procedure 23

16.0 References 24

3.0 INDEX OF FIGURES

No.	Title	Page
1	A Two-Dimensional Lifting Body Performance Steady Translation Near a Free Surface	25
2	The Prototype Problem. Flow About a Submerged Point Vortex	26
3	Free-Surface Shapes for K = +1.15 First-Order Solution, No Flat $\Delta x = 1$.	27
4	Free-Surface Shapes for K = -1.4 First-Order Solution, No Flat. $\Delta x = 1$	28
5	Free-Surface Shapes for K = +1.15 First-Order Solution. $\Delta x = 1$	29
6	Free-Surface Shapes for K = -1.4 First-Order Solution. $\Delta x = 1$	30
7	Free-Surface Shapes for K = +1.15 First-Order Solution. $\Delta x = 1$. Effect of Downstream Termination	31
8	Free-Surface Shapes for K = +1.15 First-Order Solution. $\Delta x = 0.5$ Effect of Location of Flat Termination	32
9	Nonuniqueness Study	33
10	Free-Surface Shapes for K = +1.15 Higher-Order Solution. $\Delta x = 1$	34
11	Free-Surface Shapes for K = -1.4 Higher-Order Solution. $\Delta x = 1$	35
12	Free-Surface Shapes for K = -1.7 Higher-Order Solution. $\Delta x = 1$	36
13	Free-Surface Shapes for K = -2.3 Higher-Order Solution. $\Delta x = 1$	37
14	Free-Surface Shapes for K = +1.7 Higher-Order Solution. $\Delta x = 1$	38
15	Free-Surface Shapes for K = -2.7. $\Delta x = 1$	39

4.0 PRINCIPAL NOTATION

A_{ij}, B_{ij}	respectively, the normal and tangential components of velocity at the i-th control point due to unit vorticity strength on the j-th element
g	acceleration of gravity
h	depth of submergence of a point vortex
K	strength of the point vortex. Equals $\Gamma/2\pi$
S	surface of a two-dimensional submerged body
U	freestream velocity
V	velocity along the free surface
V_{N_i}, V_{T_i}	respectively, the normal and tangential components of velocity at the i-th control point
V_{VN_i}, V_{VT_i}	respectively, the normal and tangential components of the velocity induced by a point vortex and its image (if any) at the i-th control point
x, y	respectively, horizontal and vertical coordinates
x_j, y_j	coordinates of points that define the free-surface shape. Endpoint of a surface element.
x_M	location of upstream termination of the flat
x_N	location of downstream termination of the free surface
x_O	location of downstream termination of the flat and the beginning of the normal portion of the free surface
α_i	slope angle of the i-th surface element
Δx	spacing of points along the free surface. Equals $x_{j+1} - x_j$
δ	when used in front of a quantity, denotes a small change in that quantity
Γ	circulation due to a point vortex
η	vertical location of the free surface
μ_j	vorticity strength at center of the j-th surface element
ρ	relaxation factor to aid convergence of the iterative process, equation (13)

5.0 INTRODUCTION

The problem of interest is that of the steady translation of a body in the presence of a free surface. The fluid below the free surface is inviscid and incompressible, and the flow is irrotational so that it is a potential flow governed by Laplace's equation. The fluid pressure is constant all over the free surface. In three-dimensions this problem finds its chief application in the calculation of wave resistance both for surface ships (the surface-piercing case) and for undersea vehicles (the submerged case). In two dimensions the flow about hydrofoils is the chief application. Although the problem of main practical interest is the three-dimensional one, because of its very formidable nature, the present effort has been devoted to the two-dimensional problem, where the only solution techniques considered are those with direct three-dimensional analogies.

The intention is to attempt to solve this problem in its full generality, i.e. without any assumptions of small perturbations in regard to either the body or the free surface. This is a nonlinear problem because the location of the free surface is unknown and must be solved for as part of the problem. The method of solution to be used is the surface-singularity approach (reference 1), which utilizes singularity distributions — source, dipole, vorticity — on the surface of all bodies and on the true location of the free surface. This is in contrast to small-perturbation approaches that use singularity distributions interior to the bodies and/or on the undisturbed location of the free surface. In the surface singularity approach, the strengths of these singularities are determined from the boundary conditions in terms of integral equations, which are approximated by matrix equations for numerical implementation. The singularities used are of the simple "Rankine type," which are appropriate for problems without a free surface. For example, the point source potential is $\log(1/r)$, where r is distance between the source and the point where the potential is evaluated.

6.0 GENERAL DESCRIPTION OF THE FLOW PROBLEM

It is supposed that a body is translating parallel to a free surface with uniform velocity U. By superimposing the negative of the body's translational velocity on the entire velocity field, the problem can be stated as shown in figure 1. The body surface S, which may be multiply-connected, is stationary in the presence of a uniform onset flow of magnitude U parallel to the positive x-axis. Above the body at a location $y = \eta(x)$ that must be determined is the free surface, which is a streamline of the flow along which the pressure is constant. The flow field for $y < \eta(x)$ is a potential flow, which has zero normal velocity on S and approaches the uniform freestream for $x \to -\infty$ or $y \to -\infty$. (For definiteness, the infinite-depth case is considered, but the finite-depth case could be handled by use of a single image of the body and free surface.) The undisturbed position of the free surface is $y = \eta = 0$.

If the tangential velocity at any point on the free surface is denoted V, the constant-pressure condition can be written

$$V^2 + 2g\eta = U^2 \tag{1}$$

or

$$V = \sqrt{U^2 - 2g\eta} \tag{2}$$

where g is the acceleration of gravity.

To solve this problem by a surface singularity approach, the body surface S is covered with a source density distribution. (There is also vorticity to produce circulation about S in lifting cases.) The free surface is covered with either a source or a vorticity distribution. The two distributions, i.e. on the body and the free surface, are determined from the boundary conditions on the body and free surface. However, there are three boundary conditions, i.e. zero normal velocity on S and on $y = \eta(x)$ and constant pressure on $y = \eta(x)$. Thus, two singularity distributions are insufficient, and an additional "degree of freedom" is necessary. This is the location $y = \eta(x)$, which is determined from the boundary conditions along with the source and vorticity distributions.

The surface singularity method requires that the locations of all boundaries be known. The free-surface problem must be attacked by iteration. At any stage the location of the free surface is assumed and a flow calculation is performed. Presumably one (or both) of the boundary conditions on the free surface are not satisfied. Based on some algorithm the location of the free surface is then changed, and the calculation is repeated. The above process is iterated until convergence (in some sense) is obtained. The algorithm for altering the free-surface location is highly nonunique. Many possibilities can be postulated and probably most of them lead to a divergent process. The main task in applying the surface singularity method to the free-surface problem is selection of a convergent algorithm. This is somewhat similar to the classic inverse problem, where the velocity distribution on a surface is specified and the surface shape must be computed. However, this latter problem turns out to be much simpler. Algorithms that work for it fail for the free-surface problem.

Basically the calculation can proceed in one of two general ways. At each stage it can satisfy the condition of zero normal velocity on S and on $y = \eta(x)$ and then iterate to obtain constant pressure on $y = \eta(x)$. Alternatively, at each stage it can satisfy the condition of zero normal velocity on S and the condition of constant pressure on $y = \eta(x)$ and then iterate to obtain zero normal velocity on $y = \eta(x)$. While both possibilities must be kept in mind, it is the second one that has been used successfully in inverse problems, and it has been given principal attention. Similarly either a source or a vorticity distribution may be used on the free surface. In the present work the use of a vortex distribution on the free surface has proven more effective. This is to be expected if the calculation first fixes tangential velocity as in the second alternative above, because of the powerful local effect of vorticity on local tangential velocity. However, the first alternative above was implemented using sources which have a powerful local effect on normal velocity, without success.

Strictly speaking, it is not sufficient to consider only the free surface and the body as boundaries of the problem. The domain should be closed by the addition of three more boundaries: (1) an $x = \text{constant}$ boundary at a large negative value of x on which freestream conditions (normal velocity equal to U) are prescribed; (2) a $y = \text{constant}$ boundary at a large negative value

of y on which zero normal velocity is prescribed; and (3) an x = constant boundary at a large positive value of x on which a "radiation condition" of downstream waves is applied. However, the philosophy that was followed in the present work was to try the simpler approaches first and to add complications only when these simpler approaches proved inadequate. Accordingly, the above three additional boundaries were ignored in most of the work to date. This is equivalent to the assumption that these boundaries will have weak enough sinularity strengths to give a negligible effect in the vicinity of the body. Almost certainly this is true for boundary (2).

Boundaries (1) and (3) together with the conditions applied on them imply, respectively, that no waves propagate upstream and that waves do propagate downstream. Thus, for example, if a particular calculation scheme that ignored these boundaries did not yield a wave-like free-surface shape, the inclusion of the downstream boundary (3) would be a possible remedy. As will be seen in subsequent sections, the present method does not suffer from this defect, but all forms of the method yield wave-like free surface shapes. Accordingly, the downstream boundary (3) was never considered. On the other hand, the present method does have a tendency for upstream waves to form under certain conditions, and an upstream boundary (1) was tried as a remedy. Unfortunately this attempt was not successful.

7.0 THE PROTOTYPE PROBLEM

To conserve computing time during the search for a convergent iteration algorithm, the mechanism responsible for disturbing the free surface has been taken as a submerged point vortex, as shown in Figure 2, rather than a lifting body, as shown in Figure 1. Some distance from the body its velocity field approaches that of a point vortex, so this appears to be a reasonable approximation. In any case it is known from the literature that the shape of the free surface due to a submerged point vortex is qualitatively similar to that due to a submerged lifting body. Thus, it seems likely that any proposed iteration algorithm for determining the free-surface shape would either converge for both a point vortex and a lifting body or diverge for both. The saving in computing time comes from the fact that only the free surface need be defined by surface elements. Thus, the order of the matrices that must be formed and solved is reduced. Another important reason for considering the point vortex is that this case has been considered by previous investigators, notably von Kerczek and Salvesen (references 2 and 3). Thus, solutions obtained by the present method of this report can be compared with theirs to yield an essential quantitative test of accuracy. However, it should be noted that the results of references 2 and 3 have been obtained for a finite fluid depth of 9.5 feet, so that perfect agreement with the infinite-depth results of the present method cannot be expected.

The essentials of the point vortex problem are illustrated in Figure 2. The vortex, which has a strenfth K, is located at the point $x = 0$, $y = -h$. Here $K = \Gamma/2\pi$, where Γ is the circulation. The problem has been addressed both with and without an image vortex of equal and opposite strength at the point $x = 0$, $y = +h$, and it was encouraging to note that the convergent algorithms yielded exactly the same results in both cases. During most of the work to date, an image vortex was included. All cases follow references 2 and 3 in using a freestream velocity U of 10 feet per second and a submergence depth h of 4.5 feet. Various vortex strengths K are considered, which lead to various wave heights. During most of the present effort only reference 2, not reference 3, was available. Reference 2 considers only the two vortex strengths $K = +1.15$ and $K = -1.4$. Thus most of the testing of the present method was carried out at these values of K, which are denoted

the standard vortex strengths. After a successful algorithm had been devised for these strengths, it was applied to cases having larger values of K and thus larger wave heights, for which, unfortunately, it proved less successful.

During an early stage of development of the present method the free surface was represented by a singularity distribution, source or vorticity, from x_0 to x_N (Figure 2). For a given free surface shape the singularity strengths were adjusted to satisfy one boundary condition (constant pressure or zero normal velocity) and the free-surface shape was iteratively adjusted to satisfy the other boundary condition (Section 6.0). In a later, more successful, form of the method the portion of the free surface from x_0 to x_N was treated as described above, but in addition the free surface from x_M to x_0 (Figure 2) was represented by both source and vortex singularities, whose strengths were adjusted to satisfy both boundary conditions. The portion of the free surface from x_M to x_0 was constrained to lie along the x-axis with zero normal velocity and a tangential velocity of U. The physical variables are U, h, and K. The "numerical variables" are x_M, x_0, x_N, and the element length $\Delta x = x_{j+1} - x_j$ which is used to define the free surface. In all cases presented, a constant spacing has been used, and Δx is a single number.

8.0 THE SURFACE SINGULARITY METHOD

To implement the surface singularity method of reference 1, the free surface or its approximation is represented by a set of points (x_j, y_j) as shown in Figure 2. During the course of iterating for the free-surface shape, the x_j remain fixed and the y_j are altered. The portion of the surface between two successive points (x_j, y_j) and (x_{j+1}, y_{j+1}) is a surface element on which singularity is distributed. In the "first-order" version of the method the surface element is a straight line from (x_j, y_j) to (x_{j+1}, y_{j+1}) on which the singularity is constant. In the more accurate "higher-order" version (references 1 and 4) the element is a parabola and the singularity varies linearly. Boundary conditions are applied at a single control point $(\bar{x}_j, \bar{y}_j)$ of each element, and this point is the midpoint of the element in both versions.

Although both source and vorticity distributions have been used on the portion of the free surface from x_0 to x_N, for definiteness the method is outlined below for the case when vorticity is used. This choice of singularity yields the only effective procedure. Moreover, for simplicity the case when no "flat" is employed from x_M to x_0 is described first. Let μ_j denote the vorticity strength at the control point of the jth element, and let A_{ij} and B_{ij} be, respectively, the normal and tangential components of velocity at the control point $(\bar{x}_i, \bar{y}_i)$ of the ith element due to a unit value of vorticity at the control point of the jth element. Explicit formulas for these quantities are presented in references 1 and 4 and will not be repeated here. The only difference between the A_{ij} and B_{ij} for source and vorticity distributions is that the components are interchanged with one sign changed (depending on the sign convention). Further, let V_{vNi} and V_{vTi} be, respectively, the normal and tangential components at $(\bar{x}_i, \bar{y}_i)$ due to the point vortex and its image (if any). Then the total normal and tangential components of velocity at $(\bar{x}_i, \bar{y}_i)$ are

$$V_{Ni} = \sum A_{ij}\mu_j - U \sin\alpha_i + V_{vNi} \tag{3}$$

$$V_{Ti} = \sum B_{ij}\mu_j + U \cos\alpha_i + V_{vTi} \tag{4}$$

where α_i is the slope angle of the ith element as shown in Figure 2, and where the summations are over all elements. The equations that must be satisfied are

$$V_{Ni} = 0 \tag{5}$$

$$V_{Ti} = \sqrt{U^2 - 2g\bar{y}_i} \equiv V_i(\bar{y}_i) \tag{6}$$

In the vorticity procedure the free-surface shape is assumed, and the μ_j are obtained as solutions of the simultaneous linear equations (6) with left sides given by (4), i.e. the μ_j are determined to satisfy the constant-pressure boundary condition. These values are then used in (3) to calculate normal velocities, which are not, in general, equal to zero. An iterative algorithm is then applied to alter the free-surface shape.

9.0 ITERATION ALGORITHMS

9.1 Local Algorithms

The simplest algorithm computes the change of slope angle $\delta\alpha_i$ of each element as

$$\delta\alpha_i = \tan^{-1}(V_{Ni}/V_{Ti}) \tag{7}$$

These are added to the α_i to obtain new α_i, which in turn are used to calculate new y_i successively beginning with the fixed upstream value $(x_0,0)$. Then the entire calculation is repeated. For low-slope shapes similar to a free surface, this algorithm converged for the classical inverse problem of potential flow, in which the prescribed value of tangential velocity at each $(\bar{x}_i, \bar{y}_i)$ is independent of location, but it diverges in the present application. Evidently the y-dependence of the prescribed velocity in equations (6) greatly complicates the problem.

This algorithm may be called <u>local</u> because the local slope correction is determined from the local deviation of the calculated results from the satisfaction of the boundary condition. Three such algorithms have been investigated, including one based on source singularity, and all diverged.

9.2 Global Algorithms

To obtain convergence it is necessary to employ a <u>global</u> iterative algorithm which considers the effects at <u>other</u> elements of a change in α_j and which simultaneously computes (to first order) changes in slope angle and vorticity strength that correct the normal velocities while maintaining the constant pressure condition on all elements. It should be emphasized that the final converged shape is not in any sense a small-perturbation solution. While small-perturbation formulas are used to compute shape corrections, each iteration performs a full potential-flow solution in the sense of reference 1. Thus, the converged solution has the correct normal velocity (zero) and the correct tangential velocity for constant-pressure. Deviations, if any, of the computed shape from the correct shape can only be due to nonuniqueness of the basic problem and to numerical discretization, namely the finite length of the elements and the finite locations of the x_M, x_0 and x_N.

Basically, a change of shape of the free surface affects the local velocities in four ways:

1. Rotation of the local surface through a fixed velocity field.
2. Change of vorticity strength with fixed induced-velocity matrices.
3. Change of induced-velocity matrices with fixed vorticity strengths.
4. Effect of vertical translation on vortex velocity and on the constant pressure boundary condition.

The local iterative algorithm accounts only for effect 1, while the global algorithm below accounts for effects 1, 2, and 4. Experience indicates that effect 3 may be ignored safely if surface slopes are as low as those occurring in surface wave problems.

When the free-surface shape is altered, first-order changes in the velocity components (3) and (4) are

$$\delta V_{Ni} = \sum A_{ij}\delta\mu_j - (V_{Ti} - B_{ii}\mu_i)\delta\alpha_i + \frac{\partial}{\partial \bar{y}_i}(V_{vNi})\delta\bar{y}_i \tag{8}$$

$$\delta V_{Ti} = \sum B_{ij}\delta\mu_j + V_{Ni}\delta\alpha_i + \frac{\partial}{\partial \bar{y}_i}(V_{vTi})\delta\bar{y}_i \tag{9}$$

A simple geometric calculation

$$\delta\bar{y}_i = \sum \rho_j \delta\alpha_j \tag{10}$$

expresses the first-order changes in vertical displacement in terms of slope angle changes. The conditions to be satisfied are

$$\delta V_{Ni} = -V_{Ni} \tag{11}$$

$$\delta V_{Ti} = \delta V_i(\bar{y}_i) \equiv \frac{\partial}{\partial \bar{y}_i}[V_i(\bar{y}_i)]\delta\bar{y}_i \tag{12}$$

Using (8), (9) and (10) in (11) and (12) gives a set of linear equations for $\delta\mu_j$ and $\delta\alpha_j$, the latter of which yields a new free-surface shape y_j by means of the formula

$$y_j = y_{j-1} + \Delta x \tan(\alpha_j + \rho\delta\alpha_j) \tag{13}$$
$$y_0 = 0 \qquad \text{at} \qquad x = x_0$$

where ρ is a "relaxation factor" used in some cases to improve convergence. The flow calculation is then repeated for the new shape, and an iteration is performed.

In all cases the initial approximation to the free-surface shape is the undisturbed location of the free surface $y = 0$.

10.0 FIRST-ORDER REPRESENTATION OF THE FREE SURFACE WITH NO FLAT

The initial form of the global algorithm fixed the upstream end of the free surface at $x = x_0$, $y = 0$ (Figure 2) and applied the above equations to the entire free surface from x_0 to x_N. Some of the results obtained for the free-surface shape are compared with corresponding results from reference 2 in Figures 3 and 4.

One very gratifying result is evident from these figures, namely that the present calculations yield waves. This was not at all obvious a priori. A monotonic shape might have been obtained. However, the one constantly occurring result in applying the present method is that it always gives waves, even in divergent cases. Moreover, the waves have approximately the correct wave lengths.

While the results of Figures 3 and 4 are not absurd, they are clearly unacceptable as results of a method of quantitative prediction. However, attempts to improve the results by decreasing the point spacing Δx led to divergence. In fact, any change in Δx led to divergence. The iterations only converge for $\Delta x = 1$, a clearly unacceptable situation that requires a new approach.

This approach was also implemented with sources, but it diverged immediately.

A basic problem with this approach is illustrated in Figure 4, where the solution obtained by the present method exhibits an erroneous peak at negative values of x. This occurred in all of the badly inaccurate converged cases like that of Figure 4 and also in the divergent cases. When this peak was absent, relatively accurate solutions were obtained like that of Figure 3. Thus suppression of the peak at negative values of x was pursued as the means of improving the solution. Apparently this phenomenum is related to the uniqueness question discussed in Section 6.0. Presumably, the peak at negative values of x represents a form of upstream wave propagation, which must be suppressed by applying additional boundary conditions at negative values of x.

11.0 FIRST-ORDER REPRESENTATION OF THE FREE SURFACE WITH AN INITIAL FLAT

To eliminate the peak at negative values of x and render the calculation more stable, the free surface is preceeded by an initial "flat" that is constrained to lie along the x-axis, as described in Section 7.0. Specifically, the portion of the free surface from x_M to x_0 (Figure 2) is required to lie along $y = 0$, and the tangential velocity is required to equal the freestream velocity U. The remainder of the free surface from x_0 to x_N is treated as described above. On $x_M < x < x_0$ both source density and vorticity are used to handle the two boundary conditions, and the above iterative equations are modified in that region to account for two singularity changes with no change of shape. Some cases that diverge with a short flat can be made to converge by lengthening the flat. It was found by numerical experiment that as long as the flat has the minimum length necessary to ensure convergence, further increase in the length of the flat has virtually no effect on the results. Computed results are presented for flats of sufficient length without specifically listing that length. Usually $x_M = -20$ is sufficient. Moreover, unless otherwise stated the end of the flat x_0 is at -10.

Calculated results for the two standard vortex strengths are shown in Figures 5 and 6 for a very short representation of the free surface (termination on the figure) and a unit point spacing. The wave heights agree rather well with those of reference 2, but the wave lengths are somewhat too long. Unfortunately, this solution is sensitive to the magnitude of the numerical variables. Figure 7 shows free-surface shapes calculated by the present method for three values of the downstream termination point x_N. All three calculated shapes have the same wave length (which is somewhat in error) and the same locations of peaks and zeros. However, the wave height is evidently dependent on the downstream termination point.

An effort to increase the accuracy of the calculated solution by reducing the point spacing to $\Delta x = 0.5$ is shown in Figure 8. The wave height is significantly overpredicted for the case with the flat extending to $x_0 = -10$, and again an erroneous "peak" at negative values of x is evident. Moving the flat termination to $x_0 = -5$ removes the bump and reduces the wave height, but the wave height is still incorrect and the wave length is still in error. Thus

the suppression of upstream waves is insufficient by itself. A numerical inaccuracy remains.

12.0 A NONUNIQUENESS DUE TO NUMERICAL INACCURACY

It turns out that much of the above-described sensitivity of the results to the numerical parameters is due to a nonuniqueness arising from insufficient numerical precision in the first-order formulation of the surface-singularity technique. This can be illustrated by a sample calculation. An original shape was selected that is flat from $x = -30$ to $x = -10$ and that has a wave-like shape for $x > -10$. It is shown as a solid curve in Figure 9. Flow about this shape in the presence of a uniform onset flow parallel to the x-axis was calculated using a surface source distribution and a point spacing $\Delta x = 1$. The resulting surface velocity distribution was input into a program using surface vorticity that was required to reproduce the surface velocity. If the problem had a unique solution, the resulting normal velocity distribution should be vanishingly small. Instead it was a periodic function with maximum value equal to 5% of freestream velocity. When the shape was allowed to alter itself iteratively to produce both the prescribed tangential velocity and zero normal velocity, shapes like those shown in Figure 9 were obtained for different downstream terminations. These differ from the original curve by amounts similar to those of the preceeding figure. It is not a question of the finite length of the shape, because termination at $x > 50$ give essentially the same results as that for $x = 50$ (Figure 9).

If the above procedure is carried out with the same point spacing using the higher-order version of the surface singularity technique (references 1 and 4), the magnitude of the normal velocity that expresses the degree of nonuniqueness is reduced from 5% of freestream velocity to 0.5%. Thus, with some suitable upstream point fixed, the iterated shape would be only about a tenth as far from the original shape as the iterated shapes of Figure 9. This would be quite acceptable accuracy, and it implies that use of the higher-order version is one key to quantitative accuracy of the present method.

13.0 THE HIGHER-ORDER PROCEDURE

When the higher-order surface singularity procedure of reference 4 is incorporated into the above-described global iteration procedure with initial flat, the result is a method that appears to be quite successful in predicting free-surface shapes for the two standard vortex strengths $K = +1.15$ and $K = -1.4$. Moreover, it appears to be stable with respect to the numerical parameters x_M, x_0 and x_N. Calculated results obtained with $\Delta x = 1$ are shown in Figures 10 and 11, respectively. The agreement of the wave shapes obtained by the present method with those from reference 2, is essentially exact when due account is taken of the fact that the shapes from reference 2 have been calculated for a finite depth by a numerical procedure. The curve of the present method in Figure 10 represents three graphically indistinguishable solutions obtained for the same three locations of downstream termination that are shown in Figure 7. Figure 11 shows two barely distinguishable results obtained for two downstream terminations. The calculation of Figure 10 was repeated with the flat extending to $x_0 = -6$ instead of $x_0 = -10$ as in Figure 10. The calculated free surface shape is virtually identical to that shown in Figure 10.

To investigate the dependence of the solution on the spacing Δx, the calculation for $K = +1.15$ was repeated using $\Delta x = 1.5$ and $\Delta x = 0.5$. The former gave a rather poor result with peaks 20% too low and a wave length 10% too large. The smaller spacing produced a free-surface shape that agreed very well with that of Figure 10 up to the negative peak at $x = +25$. Thereafter there is some deviation, but that could be caused by the proximity of the downstream termination at $x = +39$. This case used 138 elements on the free surface. A larger value of downstream termination could not be used because of limits on the element number imposed by computer capacity. Thus it seems reasonable to conclude that the higher-order solution is at least relatively insensitive to the numerical parameter Δx for $\Delta x \leq 1$ and that very good solutions are obtained with $\Delta x = 1$ for the two standard vortex strengths. Apparently, $\Delta x = 1.5$ is too large to give an accurate solution.

14.0 LARGER VALUES OF VORTEX STRENGTH

As stated in Section 7.0, much of the present study concentrated on the standard vortex strengths $K = +1.15$ and $K = -1.4$ because only reference 2 was available. Finally, however, not only reference 3, but a complete set of numerical results for all vortex strengths that had been considered was obtained from the authors of references 2 and 3. This permitted the present method to be tested for greater vortex strengths and greater wave heights, for which nonlinearities in the free-surface problem are more important. Calculations were performed by the present method for the following vortex strengths:

$$K = -1.7,\ -2.3,\ -2.7$$

$$K = +1.4,\ +1.7,\ +2.7$$

The strength $K = +2.7$ gives waves of such a height that the authors of references 2 and 3 feel they are on the verge of breaking.

Good results were obtained for the vortex strengths $K = -1.7$ and $K = +1.4$. The accuracy obtained and the sensitivity to the numerical parameters tested were only slightly worse than for the standard vortex strengths. This is illustrated in Figure 12 for $K = -1.7$. The wave heights are approximately 0.40 and 0.47, respectively, for $K = -1.7$ and $+1.4$.

At $K = -2.3$ some nonlinear effects are evident in the numerical solution. The free-surface wave varies from -0.48 to +0.52 after an initial peak of 0.62. The iterative procedure of the present method is less stable for this case. It is necessary to use a relaxation factor of $\rho = 1/2$ in equation (13) to obtain convergence, as opposed to the value $\rho = 1$ used for the smaller vortex strengths. Convergence to a normal velocity equal to 0.1% of freestream velocity is obtained in 10 iterations and the solution is relatively insensitive to the terminations x_M, x_0 and x_N (Figure 2). The spacing Δx was not varied. The accuracy obtained is not quite equal to that achieved at lower values of K, as is illustrated in Figure 13. It can be seen that the calculated free-surface shape erroneously rises to a value of about 0.07 immediately downstream of the flat termination of $x_0 = -10$. This is suggestive of upstream waves or of a numerical problem at the flat termination.

For $K = +1.7$ the present method encounters serious difficulty. The numerical solution yields a wave that varies from -0.54 to +0.60 after an initial peak of -0.56. As shown in Figure 14, the present method converges using a downstream termination of $x_N = +39$ and yields a fairly accurate free-surface shape for one wave cycle. The second positive peak is seriously overpredicted, and the wave length is somewhat in error. A plausible assumption would be that the downstream termination is too near the second positive peak and that increasing this parameter would lead to an improved solution. Unfortunately, every case attempted with downstream termination increased by at least one wave length proved to be divergent. Various values of the numerical parameters and the relaxation factor were tried without success. It is possibly significant that the early iterations all had sizable peaks at negative values of x, which is suggestive of upstream waves or numerical problems at the flat termination.

When the vortex strength $K = -2.7$ was used the present higher-order method diverged for all values of the numerical parameters and the relaxation factor. The first iteration for one attempt is shown in Figure 15, where it is clear that it has the proper wave-like character. Oddly the first-order procedure did converge for this case but was rather inaccurate. Both versions of the present method yield erroneous peaks at negative values of x.

For $K = +2.7$ the wave shape of the numerical solution varies from +1.25 to -0.93 and the positive and negative peaks are shapes quite differently from each other (reference 3). Convergence of the present method was not attained.

15.0 ATTEMPTS TO IMPROVE THE CALCULATION PROCEDURE

Several attempts were made to improve the calculation procedure by eliminating the peaks at negative values of x. These were of two types: alternate calculation procedures near the flat termination and an upstream boundary condition to suppress upstream waves.

Since the source strength on the free surface changes abruptly from a finite value on the flat to zero on the normal portion of the free surface, it was hoped that a smoother solution could be obtained by removing the sources and the normal velocity boundary condition. The resulting procedure diverged even for $K = +1.15$.

The higher-order procedure obtains derivatives of the singularity strengths by numerical differentiation (reference 4). Normally centered differencing is used. To eliminate a possible cause of numerical error, one-sided differences were used for the elements on either side of the flat termination. The procedure thus modified converged for the case $K = +1.15$ but gave a very poor solution.

To suppress upstream waves a vertical boundary was added at the upstream end of the flat (x_M in Figure 2). Along this boundary the downstream normal velocity was required to be equal to the freestream velocity. In one formulation the vertical extended from $y = 0$ to a large negative value of y. In a second formulation the vertical was symmetric about the x-axis and extended from a large positive value of y to an equally large negative value. Both formulations gave divergence for a vortex strength $K = +1.15$ for various values of the convergence factor.

Thus all attempts to improve the method of Section 13.0 were unsuccessful.

16.0 REFERENCES

1. Hess, J.L.: Review of Integral-Equation Techniques for Solving Potential-Flow Problems with Emphasis on the Surface-Source Method. Computer Methods in Applied Mechanics and Engineering, Vol. 5, No. 2, March 1975.

2. von Kerczek, C.H. and Salvesen, N.: Numerical Solutions of Two-Dimensional Nonlinear Wave Problems. Presented at the 10th ONR Symposium of Naval Hydrodynamics at M.I.T., June 1974.

3. Salvesen, N. and von Kerczek, C.H.: Comparison of Numerical and Perturbation Solutions of Two-Dimensional Nonlinear Water-Wave Problems. Journal of Ship Research, Vol. 20, No. 3, pp. 160-170, September 1976.

4. Hess, J.L.: Higher-Order Numerical Solution of the Integral Equation for the Two-Dimensional Neumann Problem. Computer Methods in Applied Mechanics and Engineering, Vol. 2, No. 1, February 1973.

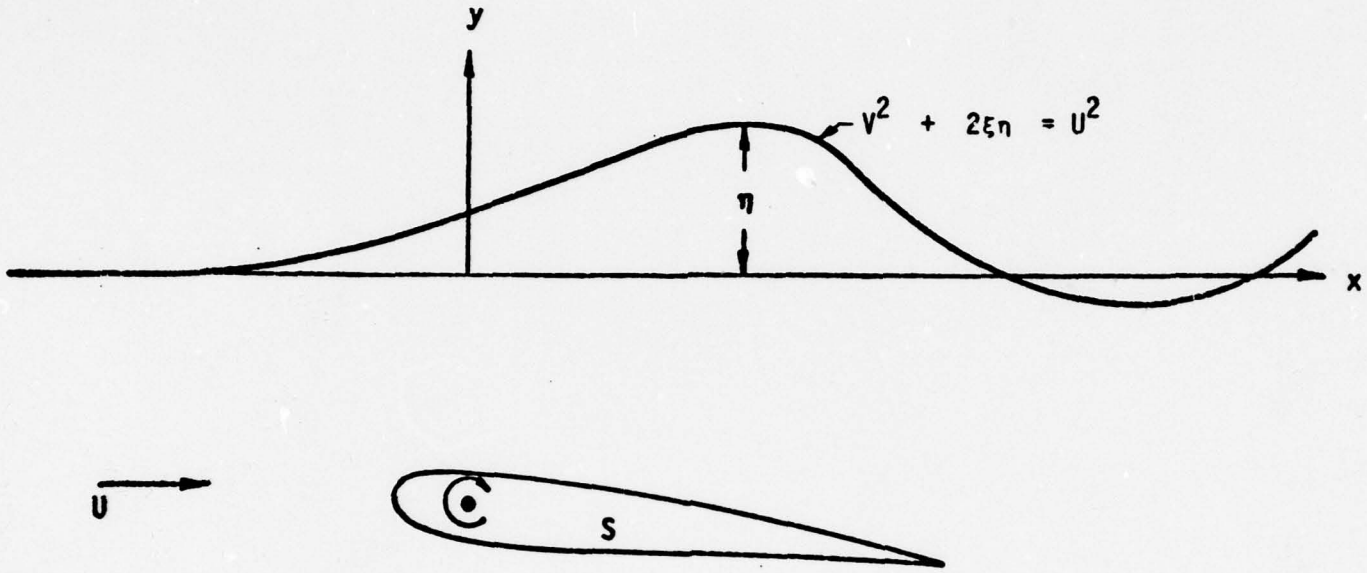

Figure 1. A Two-Dimensional Lifting Body Performing Steady Translation Near a Free Surface.

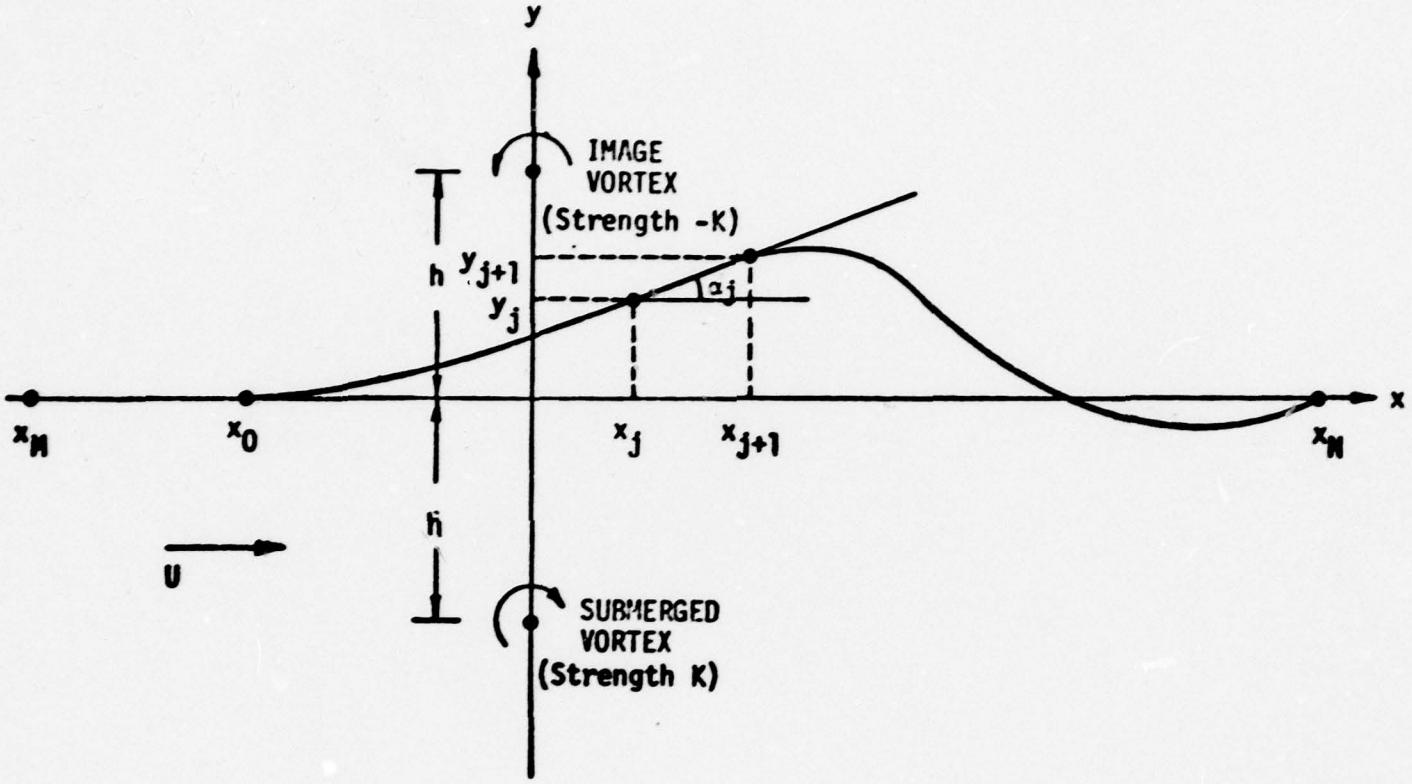

Figure 2. The Prototype Problem. Flow About a Submerged Point Vortex.

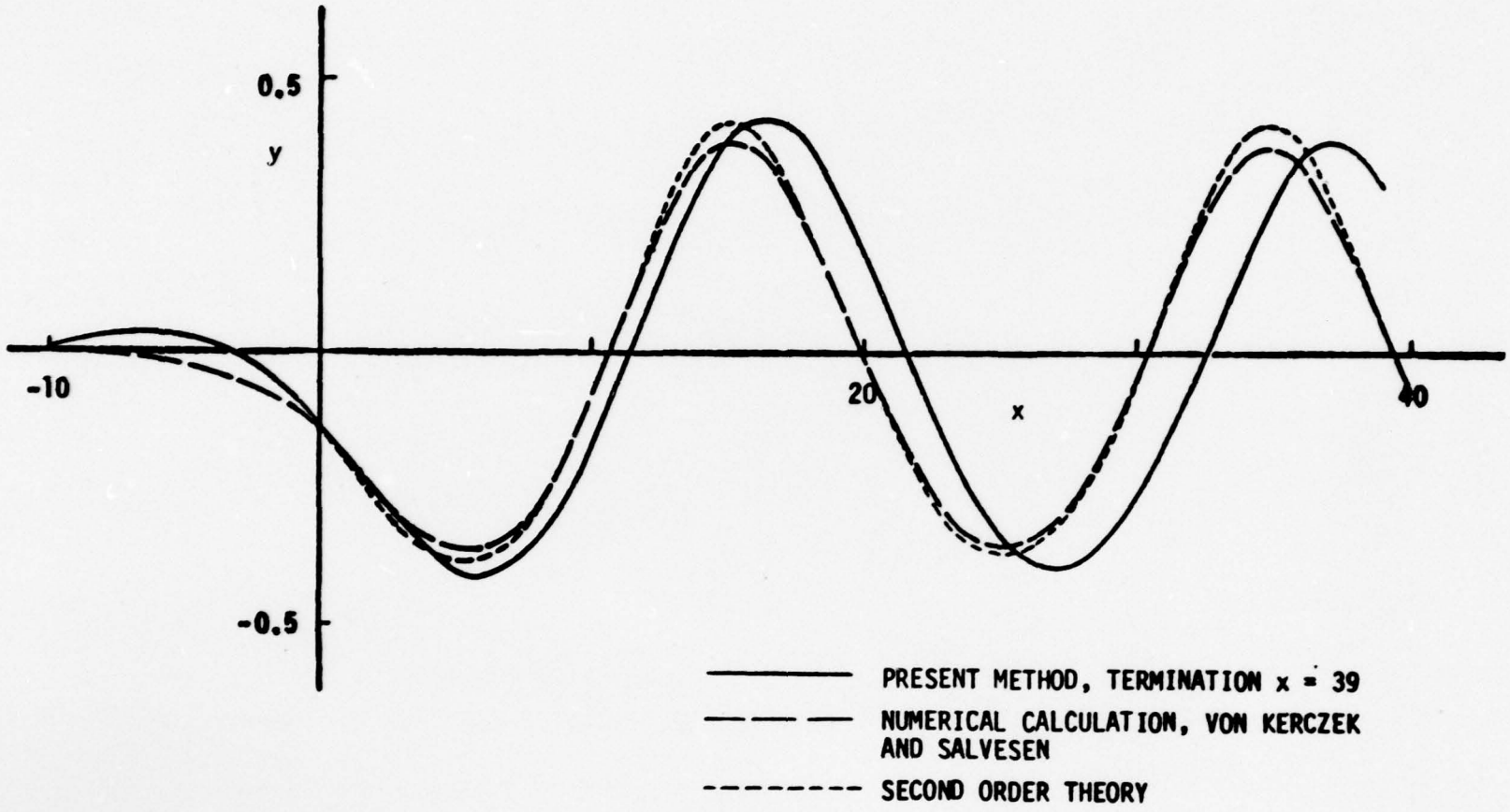

Figure 3. Free-Surface Shapes for K = +1.15 First-Order Solution, No Flat $\Delta x = 1$.

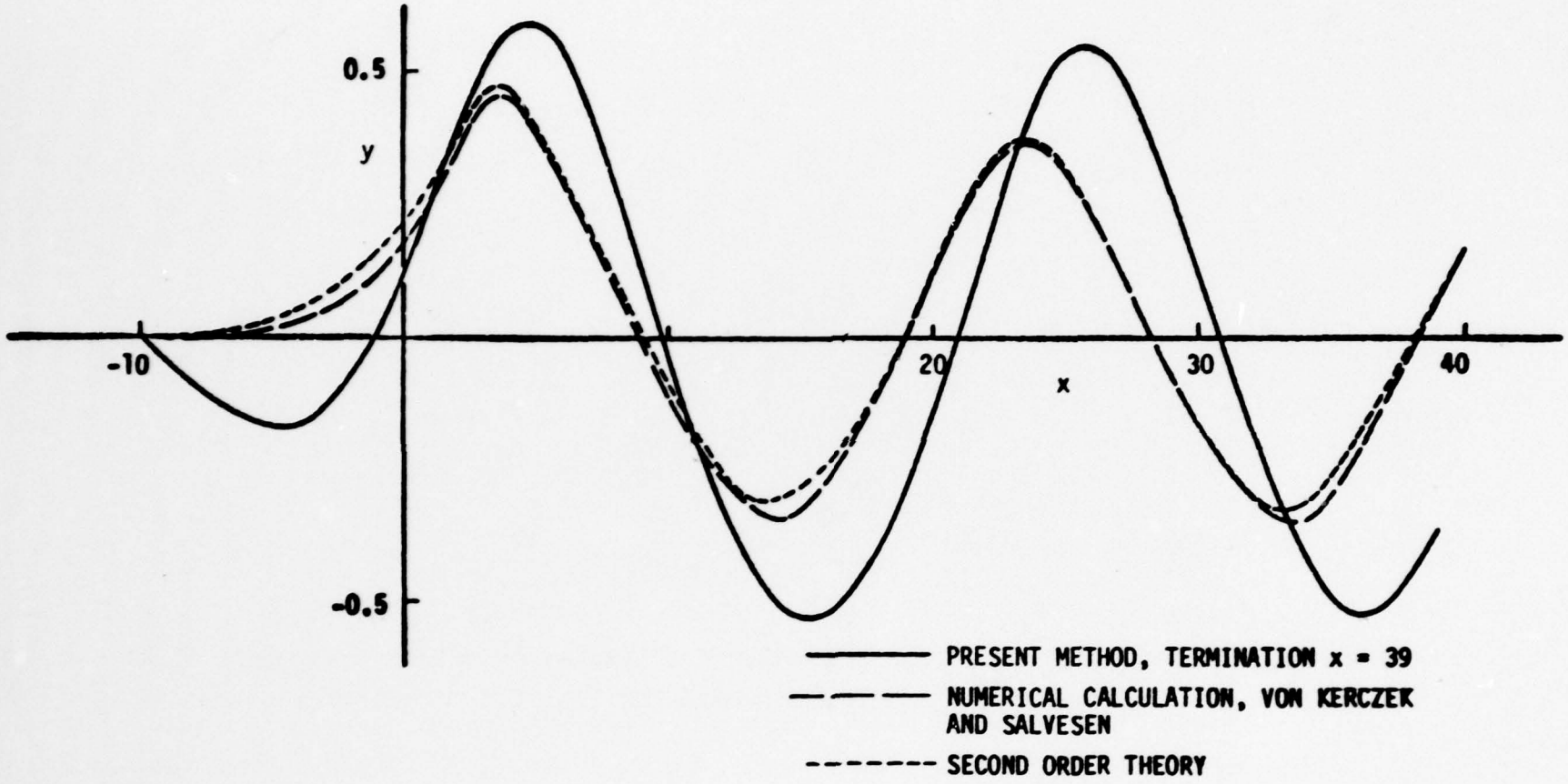

Figure 4. Free-Surface Shapes for K = -1.4 First-Order Solution, No Flat $\Delta x = 1$.

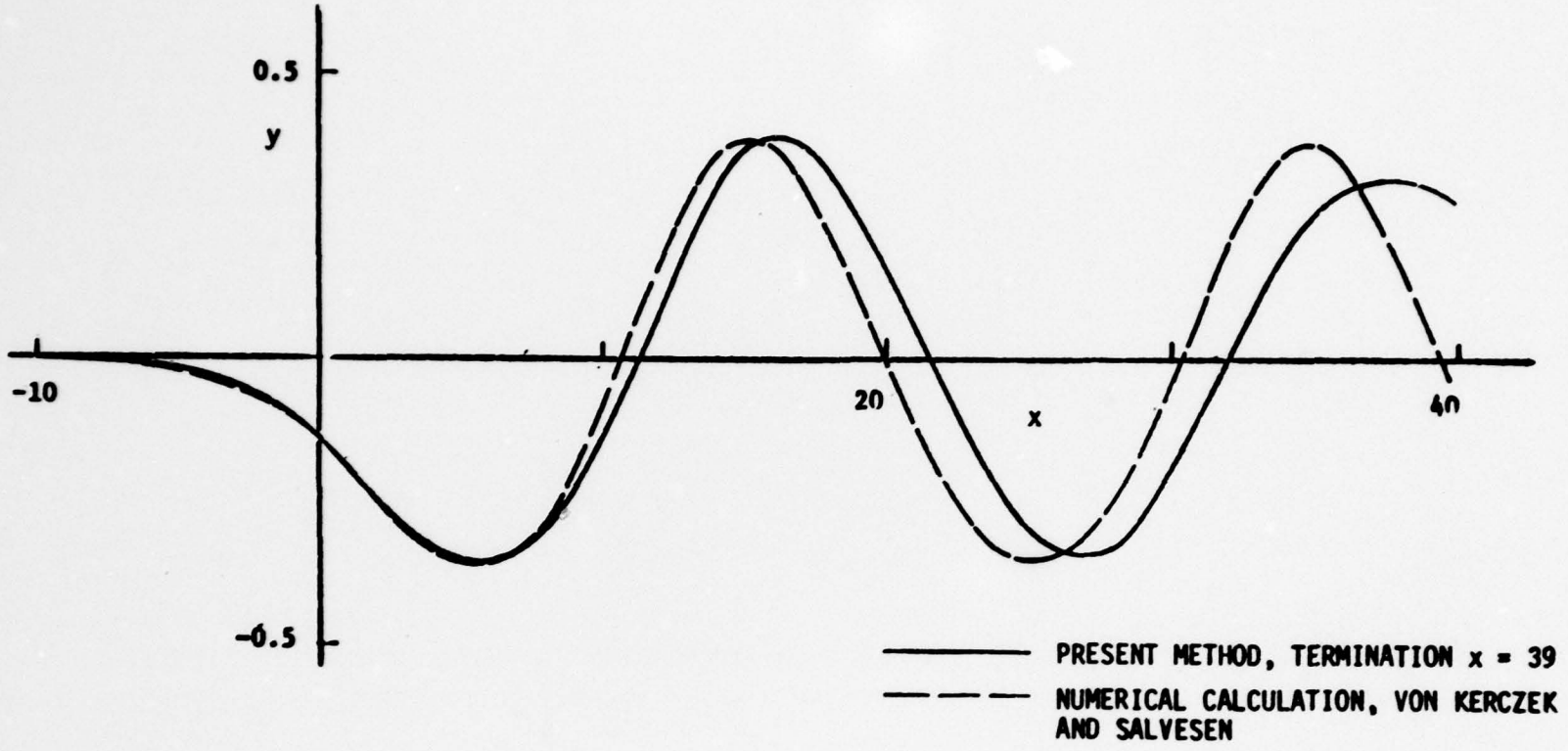

Figure 5. Free-Surface Shapes for K = +1.15 First-Order Solution. $\Delta x = 1$.

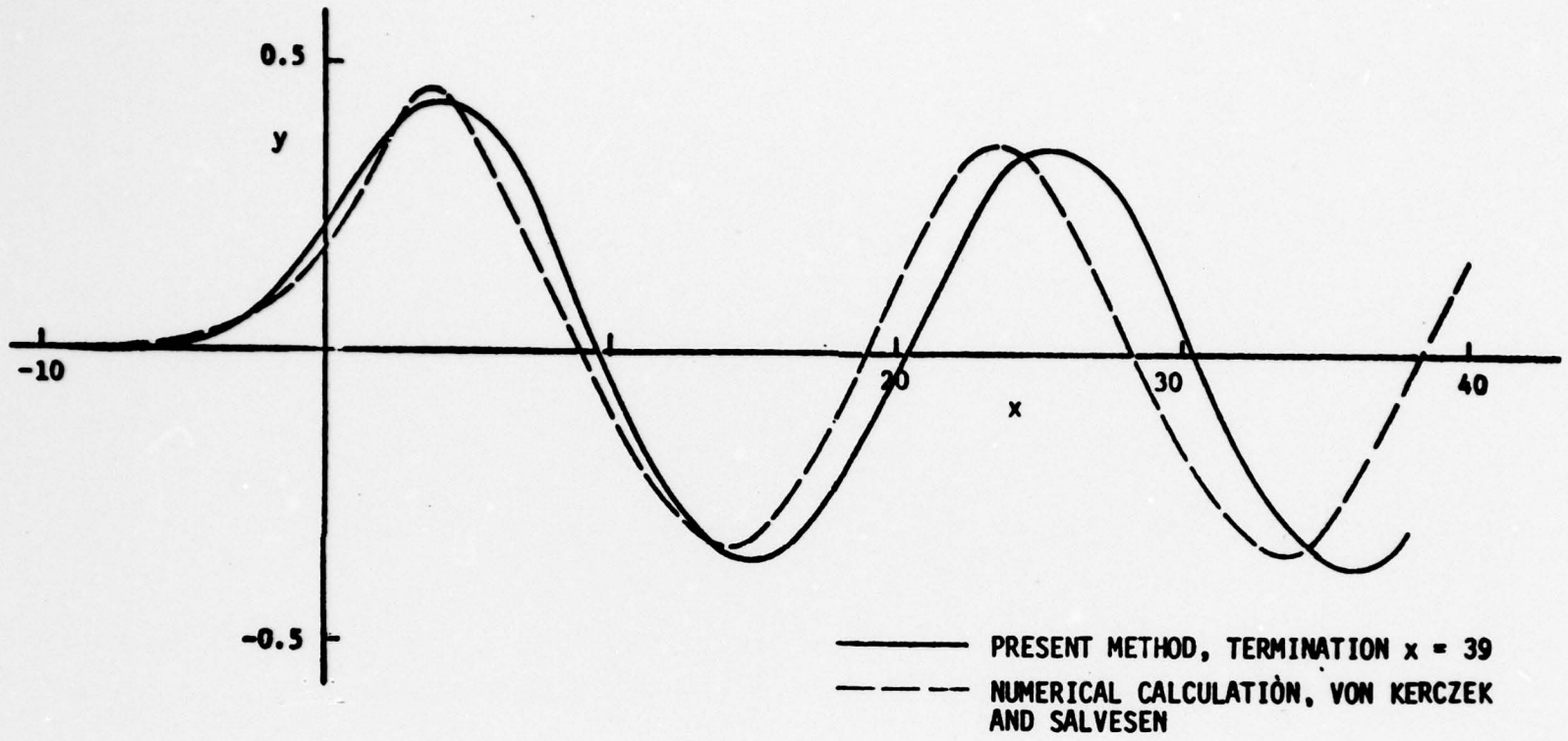

Figure 6. Free-Surface Shapes for K = -1.4 First-Order Solution. $\Delta x = 1$.

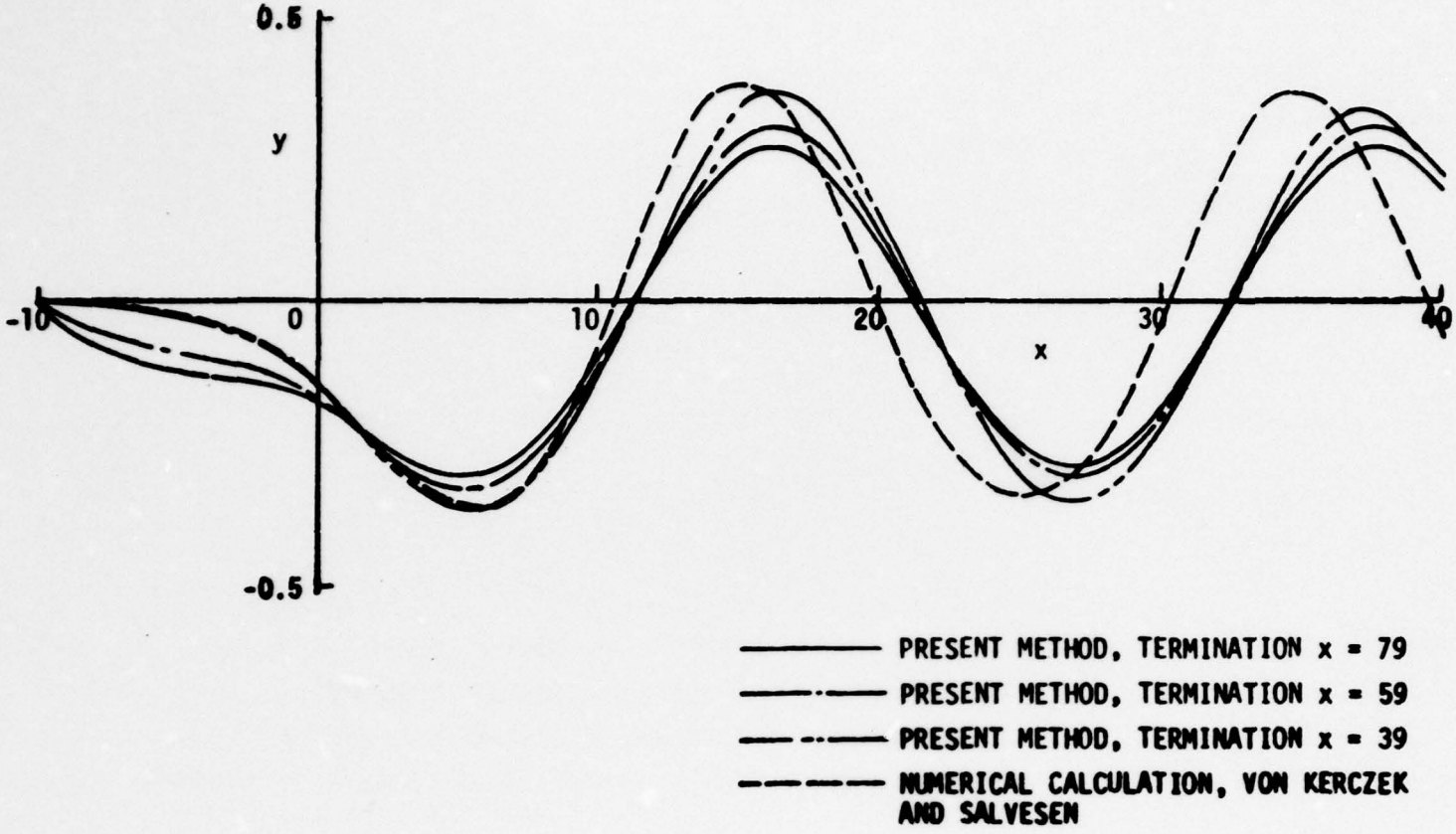

Figure 7. Free-Surface Shapes for K = +1.15 First-Order Solution. $\Delta x = 1$. Effect of Downstream Termination.

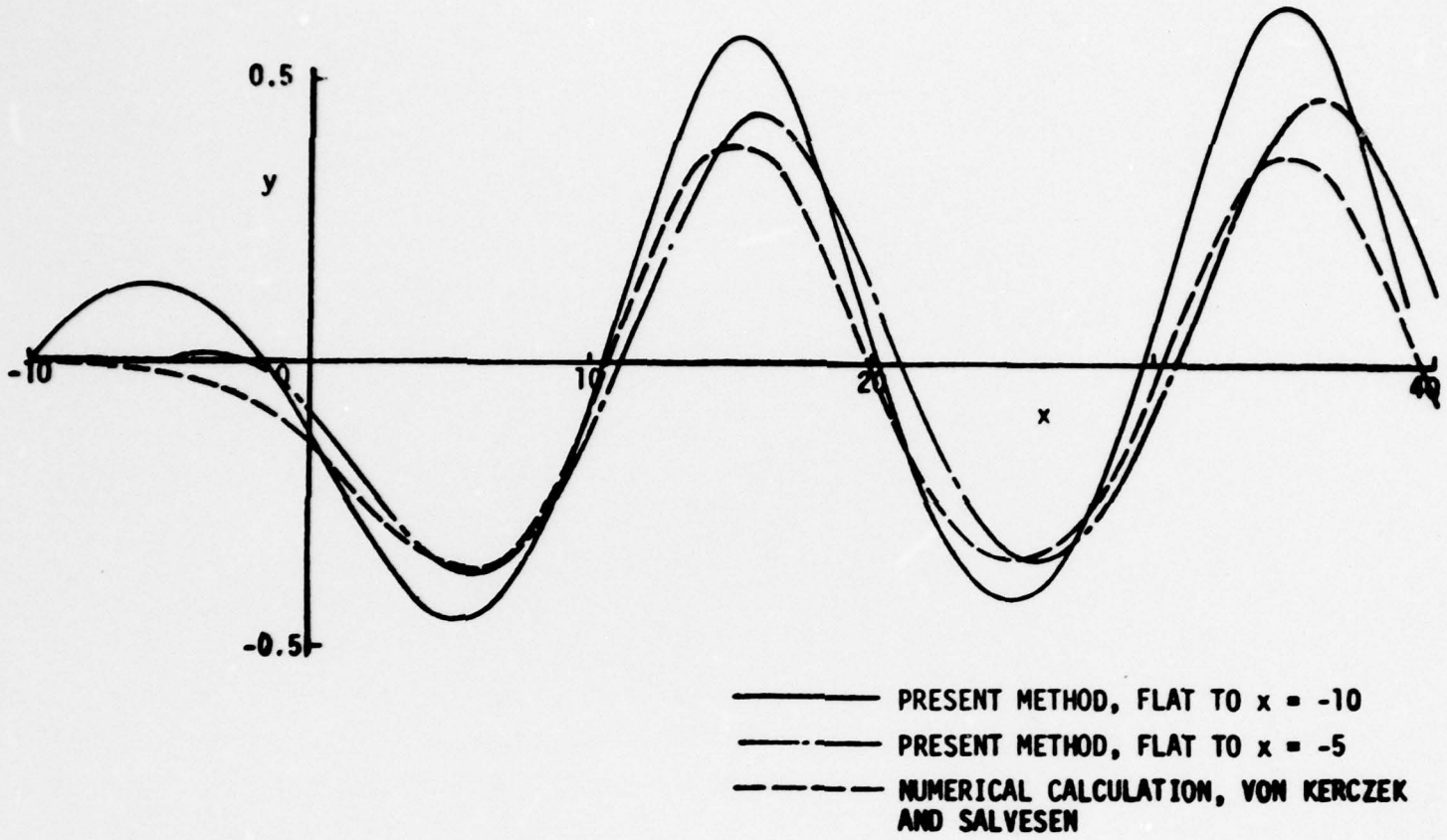

Figure 8. Free-Surface Shapes for K = +1.15 First-Order Solution. $\Delta x = 0.5$. Effect of Location of Flat Termination.

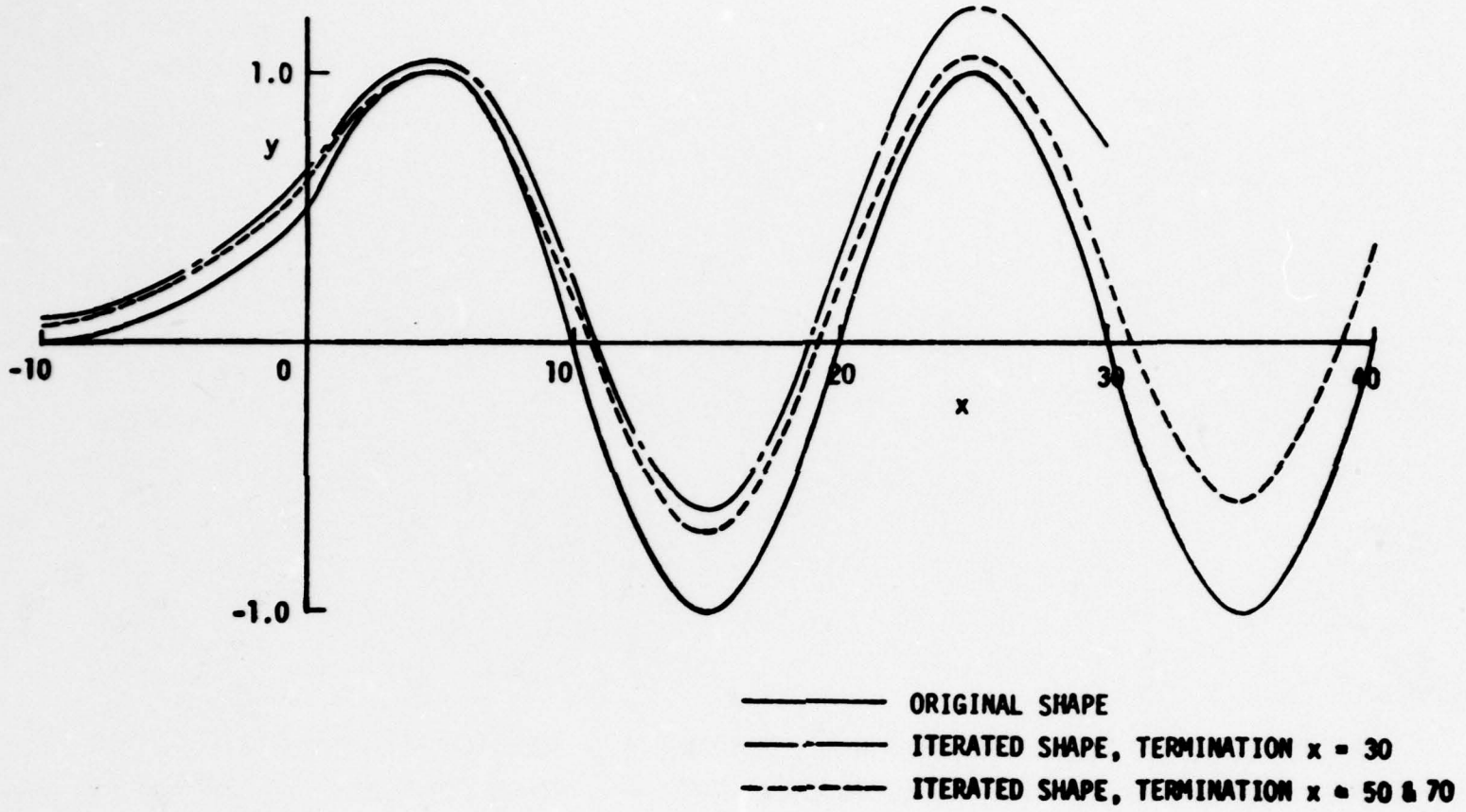

Figure 9. Nonuniqueness Study.

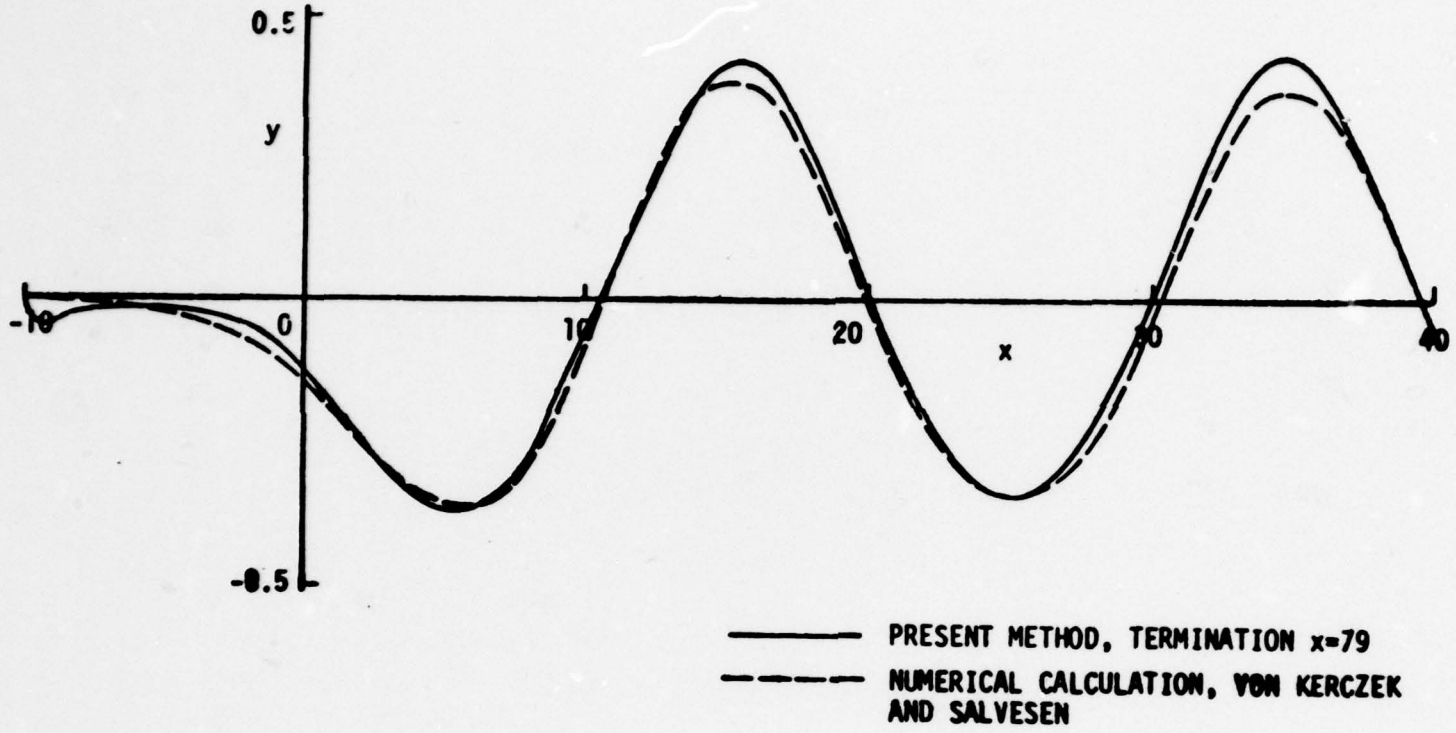

Figure 10. Free-Surface Shapes for K = +1.15 Higher-Order Solution. $\Delta x = 1$.

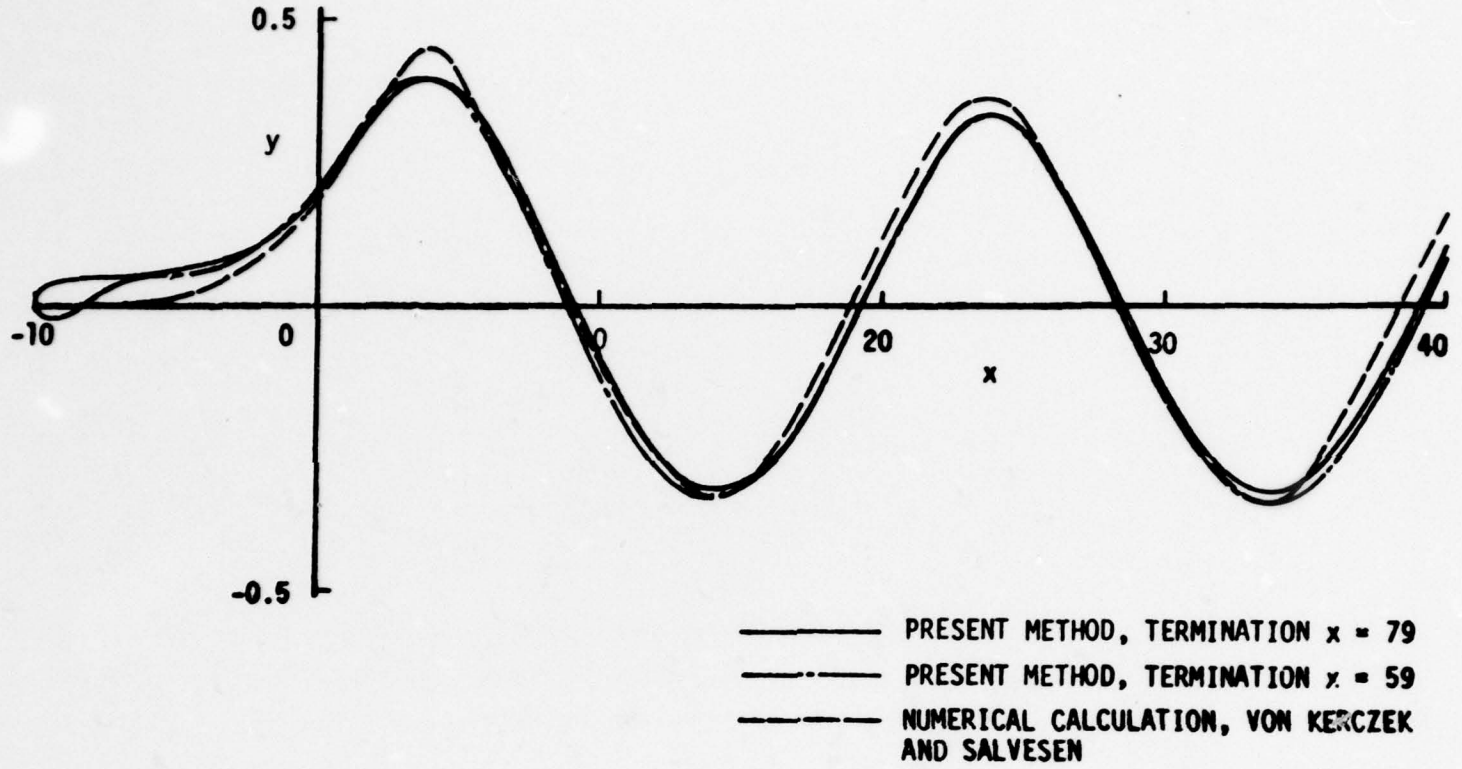

Figure 11. Free-Surface Shapes for K = -1.4 Higher-Order Solution. $\Delta x = 1$.

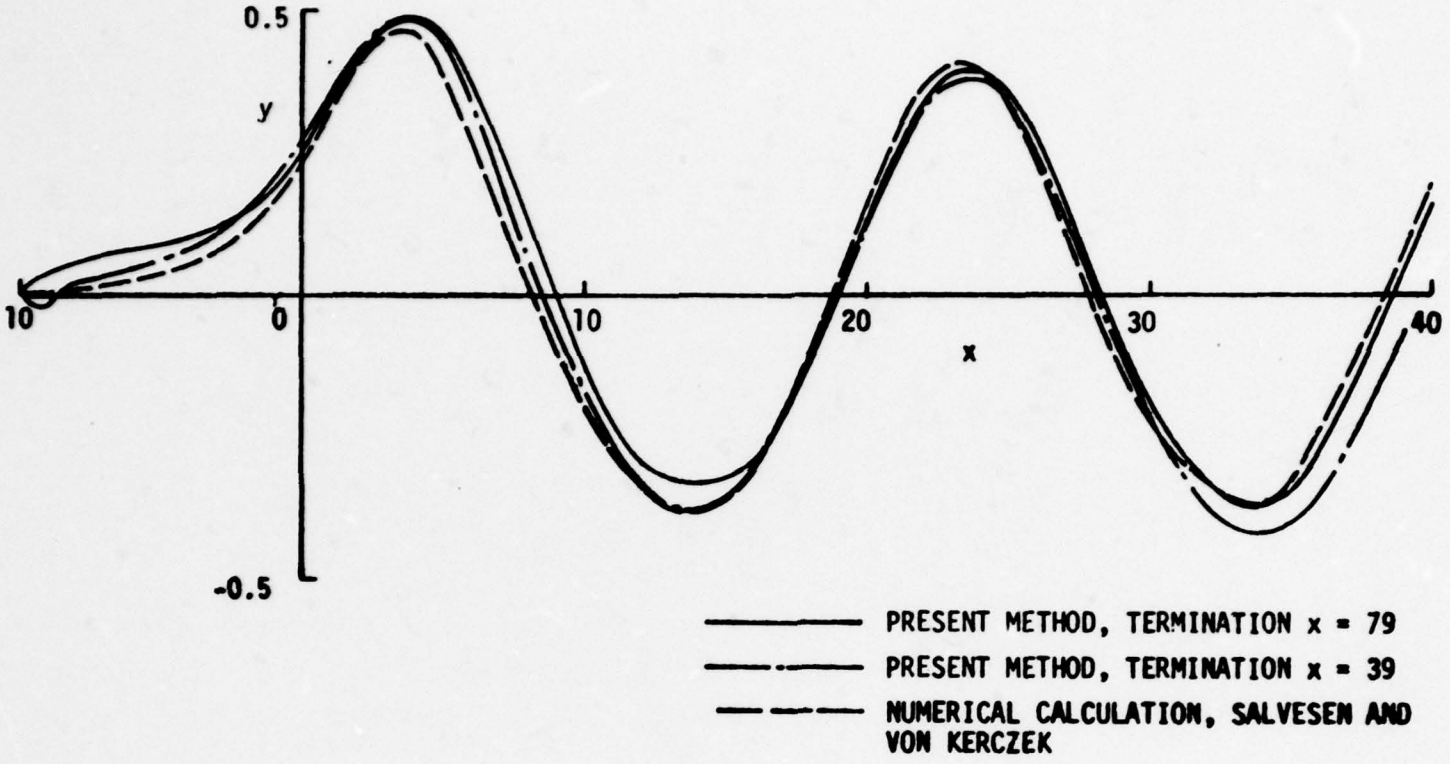

Figure 12. Free-Surface Shapes for K = -1.7 Higher-Order Solution. $\Delta x = 1$.

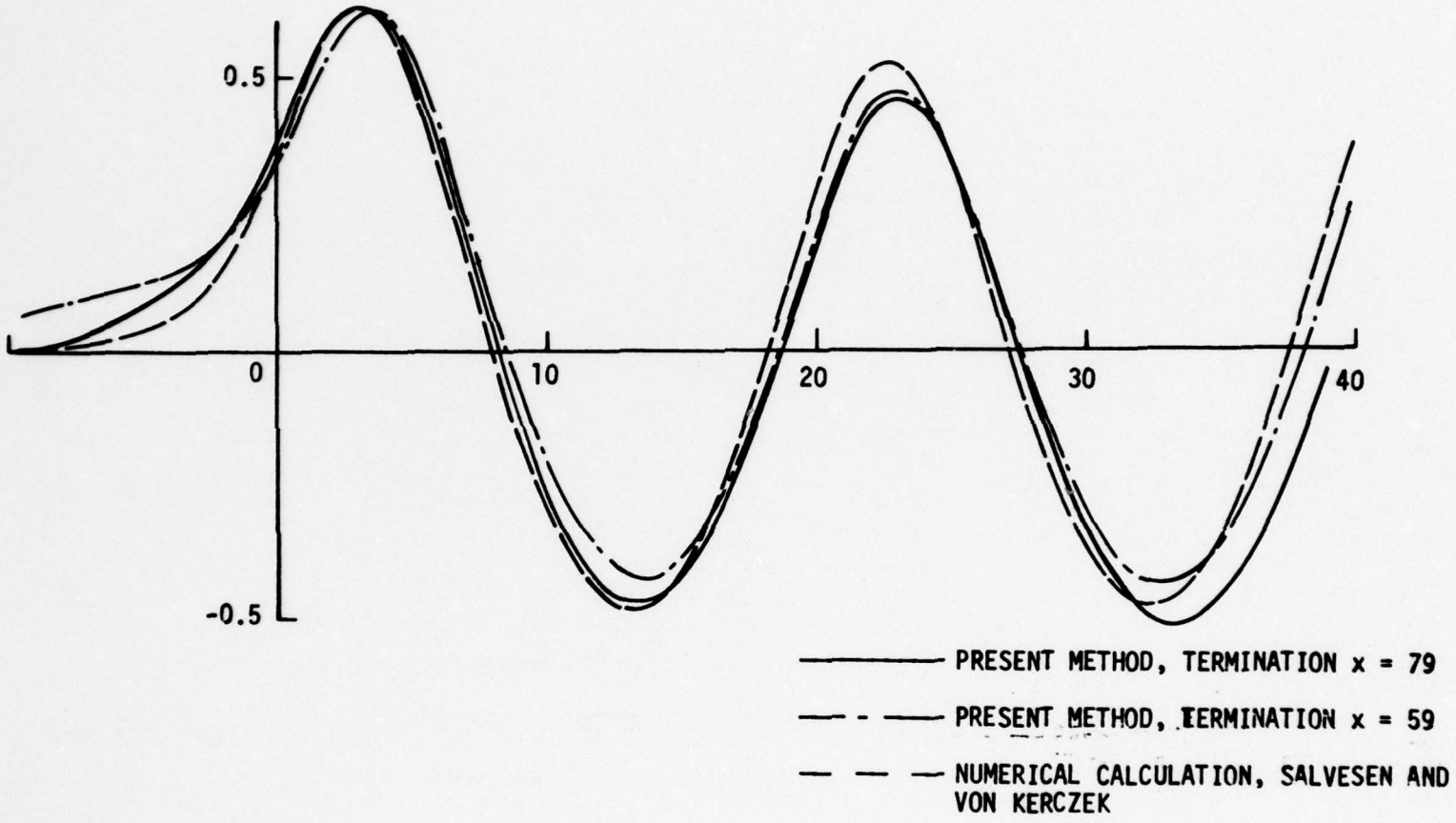

Figure 13. Free-Surface Shapes for K = -2.3 Higher-Order Solution. $\Delta x = 1$.

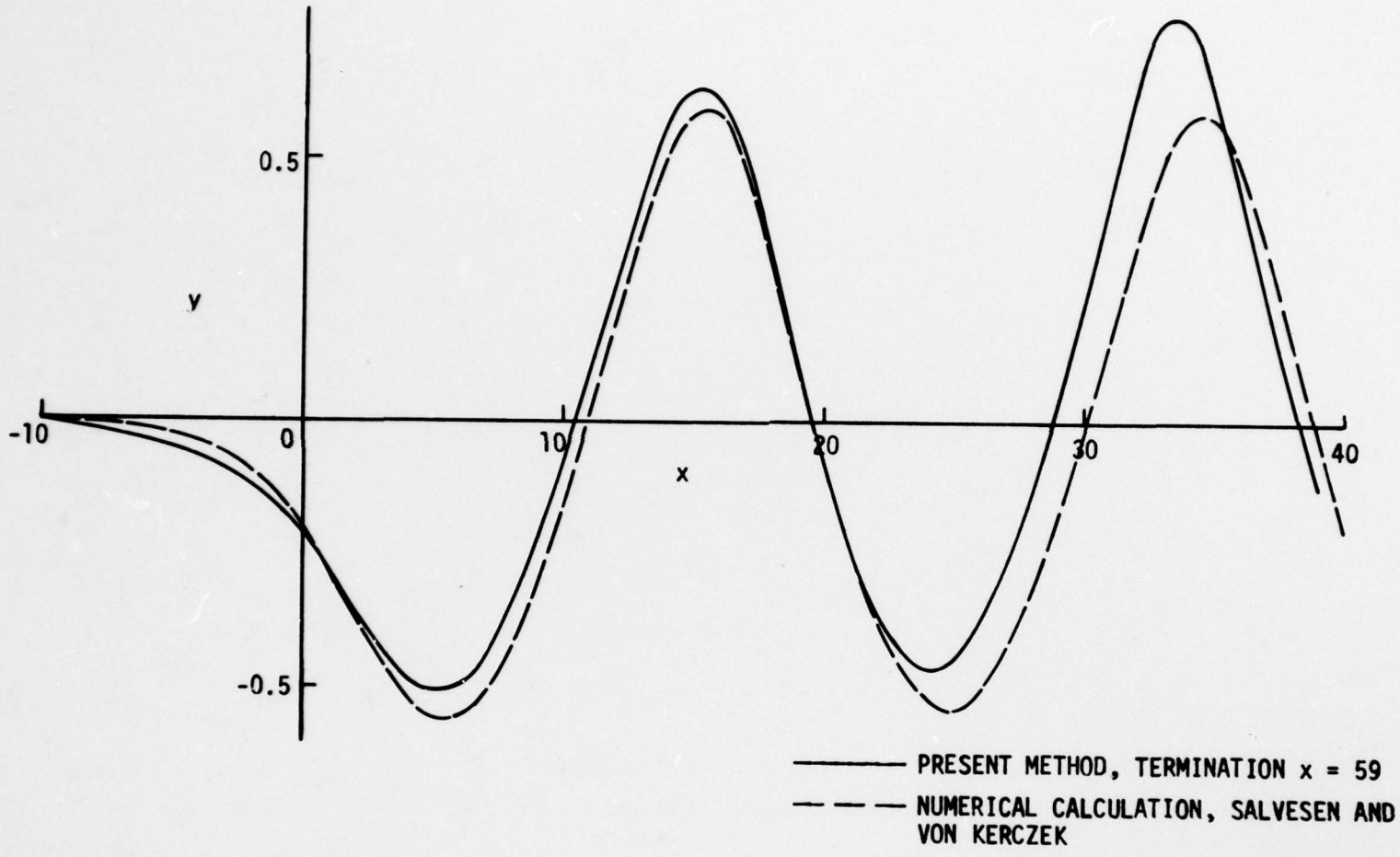

Figure 14. Free-Surface Shapes for K = +1.7 Higher-Order Solution, $\Delta x = 1$.

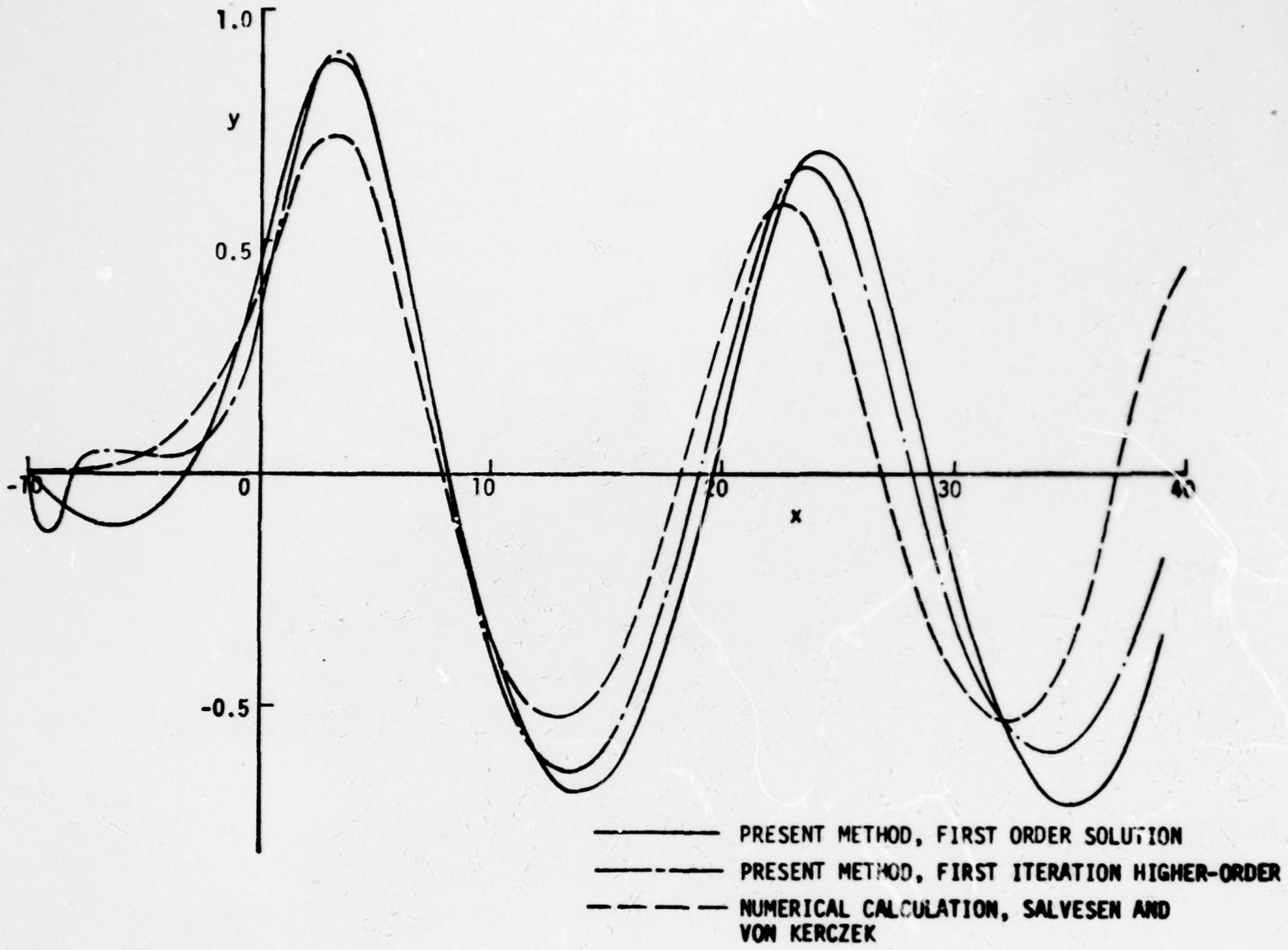

Figure 15. Free-Surface Shapes for $K = -2.7$. $\Delta x = 1$.

UNCLASSIFIED

SECURITY CLASSIFICATION OF THIS PAGE (When Data Entered)

REPORT DOCUMENTATION PAGE

READ INSTRUCTIONS BEFORE COMPLETING FORM

1. REPORT NUMBER
2. GOVT ACCESSION NO.
3. RECIPIENT'S CATALOG NUMBER

(Final)

4. TITLE (and Subtitle)

(6) ON THE SOLUTION OF NONLINEAR FREE-SURFACE PROBLEMS BY SURFACE-SINGULARITY TECHNIQUES

5. TYPE OF REPORT & PERIOD COVERED

(9) Final Technical Report, No. 2, October 1975 - January 1978

6. PERFORMING ORG. REPORT NUMBER

2

7. AUTHOR(s)

Hess, John L.

8. CONTRACT OR GRANT NUMBER(s)

(15) N00014-76-C-0337

9. PERFORMING ORGANIZATION NAME AND ADDRESS

(John L. Hess, Associates
4338 Vista Street
Long Beach, California 90803

10. PROGRAM ELEMENT, PROJECT, TASK AREA & WORK UNIT NUMBERS

(11) 10 Jul 78

11. CONTROLLING OFFICE NAME AND ADDRESS

Naval Ship Research and Development Center
Bethesda, Maryland 20084

12. REPORT DATE

July 10, 1978

13. NUMBER OF PAGES

40

14. MONITORING AGENCY NAME & ADDRESS (if different from Controlling Office)

15. SECURITY CLASS. (of this report)

15a. DECLASSIFICATION/DOWNGRADING SCHEDULE

16. DISTRIBUTION STATEMENT (of this Report)

(12) 43 p.

Approved for Public Release; Distribution Unlimited

(10) John L. Hess

17. DISTRIBUTION STATEMENT (of the abstract entered in Block 20, if different from Report)

18. SUPPLEMENTARY NOTES

19. KEY WORDS (Continue on reverse side if necessary and identify by block number)

Flow Field	Nonlinear Waves
Fluid Dynamics	Numerical Analysis
Free Surface	Potential Flow
Inverse Problem	Surface Singularity
Iterative Techniques	Surface Waves

20. ABSTRACT (Continue on reverse side if necessary and identify by block number)

This report describes an attempt to solve the two-dimensional problem of a body performing steady translation near a free surface. The aim was to solve the problem in its full generality without any linearizations or small-perturbation assumptions. The method of solution is based on iterative use of the well-known surface singularity technique and thus, if successful, the method could be generalized to three dimensions. At each stage of the procedure the free-surface shape is assumed known and the singularity strength adjusted to satisfy

Next Page

DD FORM 1 JAN 73 1473 EDITION OF 1 NOV 65 IS OBSOLETE
S/N 0102-014-6601

Unclassified

SECURITY CLASSIFICATION OF THIS PAGE (When Data Entered)

410 923

the constant-pressure boundary condition. In general, the normal velocity on the free surface is not zero. The free-surface shape is then altered by some algorithm, and the procedure is iterated to obtain zero normal velocity. The key to approach is the iterative algorithm. Various algorithms were tested by applying them to the problem of a submerged point vortex and comparing the free-surface shape obtained in convergent cases with published results. After considerable experimentation, a procedure was devised that gives very good results as long as the wave heights are not too large. For large wave heights, convergence could not be obtained, and some as yet undiscovered change in the method is needed.